Published in final edited form as:
Neuron. 2009 November 25; 64(4): 537–549. doi:10.1016/j.neuron.2009.10.005.

Endocannabinoid signaling is required for development and critical period plasticity of the whisker map in somatosensory cortex

Lu Li[*,1], **Kevin J. Bender**[*,2,‡], **Patrick J. Drew**[3], **Shantanu P. Jadhav**[4], **Emily Sylwestrak**[5], and **Daniel E. Feldman**[1,†]

[1]Dept. of Molecular and Cellular Biology and Helen Wills Neuroscience Institute, University of California Berkeley, Berkeley, CA 94720

[2]Division of Biology, University of California, San Diego, La Jolla, CA 92093

[3]Dept. of Physics, University of California, San Diego, La Jolla, CA, 92093

[4]Computational Neuroscience Program, University of California, San Diego, La Jolla, CA, 92093

[5]Neuroscience Graduate Program, University of California, San Diego, La Jolla, CA 92093

Summary

Type 1 cannabinoid (CB1) receptors mediate widespread synaptic plasticity, but how this contributes to systems-level plasticity and development in vivo is unclear. We tested whether CB1 signaling is required for development and plasticity of the whisker map in rat somatosensory cortex. Treatment with the CB1 antagonist AM251 during an early critical period for layer (L) 2/3 development (beginning postnatal day [P] 12–16) disrupted whisker map development, leading to inappropriate whisker tuning in L2/3 column edges and a blurred map. Early AM251 treatment also prevented experience-dependent plasticity in L2/3, including deprivation-induced synapse weakening and weakening of deprived whisker responses. CB1 blockade after P25 did not disrupt map development or plasticity. AM251 had no acute effect on sensory-evoked spiking, and only modestly affected field potentials, suggesting that plasticity effects were not secondary to gross activity changes. These findings implicate CB1-dependent plasticity in systems-level development and early postnatal plasticity of the whisker map.

Keywords

CB1; receptive field; AM251; barrel; rat

†Correspondence should be addressed to dfeldman@berkeley.edu.
*These authors contributed equally to this work.
‡Current Address: Oregon Hearing Research Center and Vollum Institute, Oregon Health and Science University, 3181 SW Sam Jackson Park Rd, L335A, Portland, Oregon 97239

Introduction

Type 1 cannabinoid (CB1) receptors are abundant G-protein coupled receptors (Herkenham et al., 1990; Berrendero et al. 1999) with cellular effects on synaptic plasticity, axon pathfinding, neuronal proliferation and migration (Kreitzer and Regehr, 2002; Wilson and Nicoll, 2002; Chevaleyre et al., 2006; Harkany et al., 2007). In vitro, CB1 receptors mediate multiple, widespread forms of activity-dependent short-term and long-term synaptic depression, including CB1-dependent long-term depression (CB1-LTD) at developing inhibitory and excitatory synapses. Despite the prevalence of CB1-dependent plasticity at neocortical, hippocampal, striatal, and cerebellar synapses in vitro, whether and how CB1 receptors contribute to systems-level development and plasticity in vivo is unclear.

We tested whether CB1 receptors contribute to experience-dependent development and plasticity of the whisker map in rodent primary somatosensory cortex (S1). S1 contains a topographic array of cytoarchitectonic units (barrels) in L4, each corresponding to one facial whisker and defining the boundary of a whisker-related cortical column (Woolsey and Van der Loos, 1970). L4 excitatory neurons receive thalamic whisker input and make excitatory synapses on L2/3 neurons in the same column (L4-L2/3 synapses). Virtually all L4 and L2/3 neurons respond best to deflection of the whisker corresponding anatomically to their column, resulting in a precise whisker receptive field map (Welker, 1971; Armstrong-James and Fox, 1987; Simons and Carvell, 1989; Sato et al., 2007). Whisker experience powerfully shapes the receptive field map, particularly in L2/3 (Fox, 2002), where CB1 receptors are highly expressed (Trettel and Levine, 2002; [2003]; Bodor et al., 2005; Deshmukh et al., 2007). Plasticity in L2/3 is most robust from postnatal day (P) 12–15, a period of rapid synapse formation and elaboration (Micheva and Beaulieu, 1996; Stern et al., 2001; Bender et al., 2003; Bureau et al., 2004).

While standard models of sensory map plasticity focus on NMDA receptor-dependent mechanisms (Katz and Shatz, 1996; Buonomano and Merzenich, 1998; Inan and Crair, 2007), whisker map plasticity in L2/3 during the P12–15 critical period may involve CB1-LTD at L4-L2/3 synapses (Feldman and Brecht, 2005). Whisker deprivation drives measurable LTD at L4-L2/3 synapses, which is appropriate to mediate a major component of map plasticity, the weakening of deprived whisker representations in L2/3 (Allen et al., 2003; Bender et al., 2006a). LTD at L4-L2/3 synapses in vitro is CB1-dependent (Bender et al., 2006b; Nevian & Sakmann, 2006). However, whether CB1 signaling is required for weakening of L4-L2/3 synapses and whisker map plasticity in vivo remains unknown. In addition, because CB1-LTD implements Hebbian synapse weakening (Feldman, 2000; Bender et al., 2006b), it may act to weaken inappropriate synapses during normal development of L2/3 circuits, contributing to activity-dependent development or maintenance of sharp whisker maps (Fox et al., 1996; Stern and Svoboda, 2001; Bureau et al., 2004).

Here we show, by pharmacologically blocking CB1 receptors in vivo, that CB1 receptor signaling is required for whisker map development and early critical period plasticity, including weakening of L4-L2/3 synapses. Thus, CB1-dependent plasticity is implicated in experience-dependent development of receptive fields and maps in sensory neocortex.

Results

CB1 receptors are required for whisker map development

The whisker receptive field map in adult S1 is highly precise, with ~90% of L4 neurons and ~80% of L2/3 neurons within each barrel column tuned to the anatomically corresponding whisker (Welker, 1971; Armstrong-James and Fox, 1987; Simons and Carvell, 1989; Sato et al., 2007). To characterize whisker map precision, we measured whisker receptive fields of L4

and L2/3 neurons using random interleaved deflection of 9 whiskers in a 3 × 3 array, along radial electrode penetrations in S1 of urethane-anesthetized rats. Penetration location was determined relative to barrel boundaries from marking lesions in cytochrome oxidase (CO)-stained sections (Fox, 1992), and only penetrations located within barrel columns were analyzed.

We first compared whisker receptive field maps from multiunit recordings in normal rats (normal control group, n = 7; ages P33–39), vs. rats receiving daily intraperitoneal (i.p.) injection of either vehicle (10% Tween-80 in water) or the specific CB1 antagonist AM251 (5 mg/kg in vehicle) (n = 7 rats each). Injections began on P13–16, lasted 19–21 days, and recordings were made 1 d after final injection, at ages P33–38 (Fig. 1A). AM251 crosses the blood-brain barrier, reaches peak brain concentration by 0.5–1 hr post-injection, and declines to 50% of peak concentration within 8 hours (Gatley et al., 1997). Systemic AM251 blocks CB1 receptors centrally, and is effectively cleared by 24 hr post-injection (Liu et al., 2008). The AM251 treatment period began during or soon after the critical period for rapid maturation and robust experience-dependent plasticity in L2/3 (P12–15) (Stern et al., 2001;Bender et al., 2003;Bureau et al., 2004).

Multiunit receptive fields were highly precise in control and vehicle-injected rats, as shown in a representative vehicle-treated rat (Fig. 1). Each recording penetration was localized from marking lesion or interpolation from nearby lesions to a column center (> 100 μm inside the nearest CO-stained boundary, n = 2 for this rat) or a column edge (within 0 – 100 μm of a boundary, n = 5 for this rat). In center penetrations, the percentage of recording sites in each penetration whose empirical principal whisker (PW; the whisker that evoked the most spikes over baseline) matched the anatomically appropriate whisker for the recorded column [termed P(correct tuning), calculated separately for each penetration] was 100% (Fig. 1B, C). P(correct tuning) was 75 – 100% for penetrations in column edges (Figure 1D–F). Overall, 94% of multiunit recording sites (50/53) were tuned for the anatomically correct whisker, consistent with previous single-unit recording studies (Welker, 1971;Armstrong-James and Fox, 1987;Simons and Carvell, 1989).

Receptive field precision was dramatically reduced in AM251-treated rats, as shown for an example animal in Fig. 2. While recording sites in column centers were correctly tuned for the anatomically appropriate whisker (Figure 2A, B), many sites at column edges responded best to an abnormal, anatomically inappropriate PW, and the empirical PW varied markedly across recording sites in a single penetration. For example, a penetration in the D2 whisker column (Figure 2C) contained L2/3 sites that responded best to the D1 (210, 260, 570, and 598 μm depth), E1 (320 and 369 μm), and D2 whiskers (520 μm), while L4 sites were tuned appropriately for the D2 whisker. Overall in this case, 6/7 edge penetrations were highly disrupted, with P(correct tuning) of 29%–83% (Figures 2D–F), and only 56% (32/57) of all recording sites in column edges were correctly tuned, compared with 100% (14/14) of sites in column centers.

Across all cases, whisker tuning was highly precise in control and vehicle-injected animals, and significantly degraded in AM251-treated animals (Fig. 3). To verify that inappropriate whisker tuning in AM251 treated rats was not due to accidental recording from septa-related columns, which have lower tuning precision (Alloway, 2008), we first tested whether recording penetrations were orthogonal to the cortical surface (6 penetrations, 3 rats). In each penetration, 2 marking lesions were made and subsequently visualized in coronal CO-stained sections. The angle between the penetration trajectory (from lesion interpolation) and the tangential plane defined by L4 barrel centers was 90.1 ± 0.76 degrees [range: 88.0 – 93.1 degrees] (Figure S1). Second, we confirmed that whisker tuning was equally disrupted in AM251-treated rats in penetrations that were directly marked with lesions, vs. penetrations whose location was

triangulated from nearby lesions, indicating that tuning abnormality was not an artifact of triangulation errors (Figure S2).

Laminar and column edge specificity of whisker map disruption

To quantify map disruption, we calculated P(correct tuning) for each penetration in vehicle-treated, uninjected control, and AM251-treated animals (n = 38, 20, and 38 penetrations, respectively). Median P(correct tuning) was 100% in uninjected controls and 88% in vehicle-injected rats (NS, $p = 0.30$, Wilcoxon test). AM251 treatment decreased median P(correct tuning) to 60% ($p < 0.01$ vs. vehicle and control groups, Wilcoxon test) (Figure 4A–B, "all"). Tangential distribution and depth of recording sites within columns were identical between AM251 and vehicle animals (Figure S3).

Map disruption was most prominent in L2/3, and less, but still significant, in L4 (Fig. 4B). This parallels the laminar distribution of CB1 expression (Bodor et al., 2005;Deshmukh et al., 2007;Liu et al., 2008). Median P(correct tuning) for L2/3 sites was 55% in AM251 rats vs. 100% in vehicle rats ($p < 0.01$, Wilcoxon test), and for L4 sites was 75% vs. 100% ($p < 0.01$). Within each penetration in AM251 cases, the proportion of correctly tuned recording sites was significantly lower in L2/3 than in L4 (55% vs. 75%, n = 38, $p < 0.01$, paired Wilcoxon test). Overall, 39% (62/159) of L2/3 sites and 66% (89/135) of L4 sites showed a correct PW in AM251 treated animals, compared to 81% (92/113) and 83% (133/161) of sites in vehicle-treated animals.

Map disruption was restricted to column edges. For each penetration, we plotted P(correct tuning) versus the distance to the nearest CO-stained barrel boundary (Figure 4C). Penetrations closest to the barrel edge were most disrupted by AM251. In AM251 cases, a sliding Wilcoxon test identified a significant delimiting boundary separating regions of high- and low-P(correct tuning) at 100 μm from the barrel edge. This finding justifies the use of 100 μm to separate center from edge, above. Penetrations outside this boundary had significantly lower P(correct tuning) (median 57%, n = 31 penetrations) than penetrations central to this boundary (100%, n = 7, $p < 0.05$) (Figure 4C). The disorganized edge region occupied a substantial fraction of the cortical column (42% of column area, assuming an idealized 450 × 400 μm column). Within column edges, L2/3 was maximally disrupted, with median P(correct tuning) reduced from 100% in vehicle cases to 33% in AM251 cases (Wilcoxon test, $p < 0.006$). In contrast, L4 was less disrupted, with median P(correct tuning) reduced from 100% in vehicle cases to 75% in AM251 cases, $p < 0.03$). Neither L2/3 nor L4 was disordered in column centers (Fig. 4D).

To remove any confounding effects of irregular barrel column shape on center-edge analysis, we analyzed P(correct tuning) after transforming penetration locations to a standard rectangular coordinate frame. Results confirmed that whisker tuning was selectively and powerfully disrupted in column edges (see Supplemental Material and Figure S4B–C). Moreover, there were no systematic differences in P(correct tuning) in arc- vs. row-facing quadrants of barrel columns (n = 18, 20; $p < 0.20$, Wilcoxon test), suggesting that disorganization was isotropic on average (Figure S4D). Thus, blockade of CB1 signaling during weeks 2–4 of postnatal development severely reduces whisker map precision at barrel column edges, particularly in L2/3, as measured by multiunit whisker tuning.

Disruption of single-unit receptive fields

In separate experiments, we measured how AM251 disrupted whisker tuning of isolated single units, recorded specifically in the edges of the D2 and C2 whisker columns. In control-and vehicle treated animals (considered together, n = 4), 94% (16/17) of L2/3 single units and 86% (6/7) of L4 single units responded best to the anatomically appropriate PW. In AM251-treated rats, only 34% (13/38) of L2/3 units responded best to the anatomically appropriate PW, while

66% responded best to an inappropriate neighboring whisker (e.g., D3, Fig. 5A–C). In contrast, 77% (10/13) of L4 neurons were appropriately tuned. AM251 treatment caused receptive field sharpness (PW response / mean response to the 8 immediate surround whiskers) to decrease by 23% in L2/3 (from 5.0 ± 0.4, n = 13, to 3.9 ± 0.3, n = 23, $p < 0.04$, t-test), indicating that whisker tuning was broader in AM251-treated vs. control rats. Sharpness remained unchanged in L4 (AM251: 4.8 ± 1.8, n = 6; vehicle/control: 4.5 ± 0.9, n = 7, $p < 0.86$, t-test) (Fig. 5D). At 8/16 recording sites in AM251 cases, neighboring single units isolated from the same recording site were tuned to different whiskers, indicating that receptive field disorganization occurred at a fine spatial scale within column edges.

Deflection of the anatomically appropriate whisker evoked 0.76 ± 0.17 spikes stimulus^{-1} from L2/3 single units in vehicle/control cases (n = 17 neurons), and 0.53 ± 0.13 spikes stimulus^{-1} from mistuned neurons in AM251 cases (n = 25 neurons), which was not significantly different ($p < 0.29$, t-test). In contrast, the response to the strongest surround whisker in vehicle/control cases was 0.47 ± 0.09 spikes stimulus-1, while the response to the empirical (inappropriate) best whisker in AM251 cases was significantly greater, 0.78 ± 0.14 spikes stimulus^{-1} ($p < 0.03$, t-test) (Fig. 5F). Thus, inappropriate tuning in AM251 cases was caused, at least in part, by overly strong responses to inappropriate surround whiskers.

Analysis of response time course showed that mistuned neurons in AM251 cases responded to their incorrect principal whisker with a time course and modal latency (median 20 ms) indistinguishable from normal surround responses in control/vehicle cases (21 ms, $p < 0.84$) (Fig. S7). This suggests that responses to inappropriate whiskers were mediated though circuits that normally mediate surround whisker responses. Mistuned neurons responded to the anatomically appropriate whisker with a time course similar to that of normal PW responses in control/vehicle cases, but a slightly longer latency (13 vs. 16 ms, $p < 0.01$).

Whisker map blurring confirmed by intrinsic signal optical imaging

The development of inappropriate whisker responses in AM251-treated animals suggests that whisker representations overlap more, thus blurring the whisker map. To test this hypothesis, we performed intrinsic signal optical imaging to measure the extent of functional S1 columns activated by E2, D2, and C2 whiskers (Chen-Bee et al., 2000; Drew and Feldman, 2008). Results showed that in AM251 cases, individual whiskers activated larger areas in S1, and that functional representations of adjacent whiskers overlapped more than in control/vehicle cases (see Supplemental Material and Figure S5). Because intrinsic signal imaging primarily reflects neural activity in L2/3, these results demonstrate that L2/3 whisker maps were blurred, and individual whisker representations enlarged, in AM251-treated animals.

CB1 receptors are required for experience-dependent synapse weakening

Whisker disuse drives a presynaptic form of LTD at L4-L2/3 excitatory synapses onto L2/3 pyramidal neurons in vivo, which can be detected in brain slices prepared from whisker-deprived animals (Allen et al., 2003; Takahashi et al., 2003; Bender et al., 2006a). In vitro, LTD at L4-L2/3 synapses is CB1-dependent and expressed by a decrease in presynaptic release probability (Bender et al., 2006b; Nevian and Sakmann, 2006). Both deprivation-induced synapse weakening in vivo and acute LTD in vitro cause an increase in paired pulse ratio (PPR), defined as the ratio of two sequential postsynaptic currents (EPSC2/EPSC1; PPR < 1.0 signifies paired pulse depression) (Bender et al., 2006a; Bender et al., 2006b). PPR is inversely related to presynaptic release probability at many synapses (Dobrunz and Stevens, 1997; Zucker and Regehr, 2002). Thus, whisker deprivation has been proposed to weaken L4-L2/3 synapses via CB1-LTD, and this synapse weakening may underlie weakening of deprived whisker representations in L2/3 in vivo (Allen et al., 2003; Feldman and Brecht, 2005).

To test whether CB1 signaling is required for experience-dependent weakening of L4-L2/3 synapses in vivo, we plucked the D-row whiskers for 3 d, beginning at P16–19, and administered daily injections of either AM251 (10 mg/kg, i.p.) or vehicle, or gave no injections. We then prepared "across-row" S1 slices, and measured PPR at presumptive L4-L2/3 synapses in D and B columns within the same slice. These columns can be identified unambiguously in these slices (Allen et al., 2003) (Fig. 6A). PPR was measured for pharmacologically isolated AMPA receptor-mediated excitatory postsynaptic currents (EPSCs), recorded in whole-cell voltage clamp from L2/3 pyramidal cells, in response to extracellular L4 stimulation. We chose 3 days deprivation because it is the minimum required to increase PPR at L4-L2/3 synapses, allowing us to characterize CB1 involvement in rapid plasticity. All recordings were made at P19–22.

In vehicle-injected, non-whisker-deprived rats (Figs. 6B, C, "whiskers intact"), L4-L2/3 EPSCs showed equivalent, modest paired pulse depression (40 ms interval) in both D and B columns (D-row PPR: 0.95 ± 0.03, n = 16; B-row: 0.97 ± 0.04, n = 12; $p > 0.5$), consistent with prior studies (Bender et al., 2006a; Feldmeyer et al., 2002). PPR did not vary with age over the P19–22 measurement period (ANOVA $p = 0.74$). D-row deprivation in uninjected rats (n = 6 rats) significantly increased PPR in deprived D columns relative to spared B columns of the same slices (D-row: 1.32 ± 0.06, n = 23; B-row: 1.00 ± 0.07, n = 6; $p < 0.05$, t-test) (Figs. 6B, C), similar to a previous study using 7 d of deprivation (Bender et al., 2006a) (data replotted here as "7 d dep", Fig. 6C). AM251 treatment during the deprivation period completely prevented the deprivation-induced increase in PPR in deprived columns (D-row: 0.95 ± 0.3, n = 16: B-row: 0.97 ± 0.04, n = 12; $p > 0.5$), while vehicle injections did not prevent the effect (D-row: 1.35 ± 0.09, n = 13; B-row: 0.91 ± 0.04, n = 6; $p < 0.005$, unpaired t-test). Thus, CB1 signaling is required for deprivation-induced, presynaptic weakening of L4-L2/3 synapses.

CB1 signaling is required for depression of whisker-evoked potentials in vivo

To test whether CB1 signaling is required for weakening of deprived whisker representations in L2/3 in vivo, we measured whisker-evoked sensory responses in urethane-anesthetized rats using whisker-evoked local field potential recordings (WEPs). WEPs were recorded with a glass pipette 400, 800, and 1000 μm below the pia, corresponding to L2/3, L4, and L5a (Celikel et al., 2004), with WEP electrode tip size and resistance carefully matched between experiments (Fig. 7). WEPs are thought to reflect average subthreshold synaptic responses from nearby neurons, analogous to visually evoked potentials (VEPs) used to characterize plasticity in the rodent visual system (Sawtell et al., 2003). We used WEPs to characterize rapid whisker response plasticity in vivo because 3 days of whisker deprivation is sufficient to depress WEPs, but longer deprivation is necessary to significantly depress single-unit responses to deprived whiskers (data not shown). Recordings were targeted to the center of D1 or D2 columns by intrinsic signal optical imaging, with recording location verified post-hoc relative to CO-stained barrel boundaries (see Supplemental Data).

In control rats with normal whisker experience, principal whisker deflection (2° amplitude, 4 ms ramp, 100 ms hold, rostral deflection) evoked strong negative WEPs in L2/3 and L4, with L4 WEPs having higher amplitude and faster rise than L2/3 or L5a WEPs (L2/3: −0.66 ± 0.11 mV amplitude, n = 8; L4: −0.81 ± 0.13 mV, n = 8; L5a: −0.70 ± 0.11 mV, n = 8; all WEPs recorded at P22–25) (Fig. 7). In rats with D-row whiskers trimmed for 3 days beginning on P19–22 (72 hr prior to recording), L2/3 WEPs (evoked by deflection of the regrown whisker stub) were reduced in amplitude by 53% relative to neighboring, undeprived columns (deprived D columns: −0.37 ± 0.12 mV, n = 8; spared C1, C2, and E2 columns: −0.79 ± 0.06 mV, n = 7, $p < 0.0001$, t-test) and by 39% relative to D columns in undeprived control littermates ($p < 0.05$, t-test). L4 WEPs showed a non-significant trend toward reduction relative to neighboring spared columns (deprived D columns: −0.59 ± 0.08 mV, n = 8; spared non-D column in the

same animals: −0.77 ± 0.1, n = 7, p = 0.13) and compared to D columns in non-deprived littermates (p = 0.18, t-test). Deprivation did not reduce WEPs in L5a (deprived D columns: −0.73 ± 0.14 mV, n = 8). This laminar profile is consistent with weakening of deprived whisker responses primarily in L2/3, and less in L4, as observed for whisker-evoked spiking in D-row deprived rats (Drew and Feldman, 2008).

In D-row trimmed rats injected daily with AM251 (10 mg/kg), WEP amplitude was identical to whisker-intact controls (L2/3: −0.60 ± 0.05 mV, n = 8, p > 0.05 vs. control; L4: −0.87 ± 0.14 mV, n = 8, p > 0.05 vs. control; L5a: −0.72 ± 0.12 mV, n = 8, p> 0.05 vs. control), and the reduction in WEP amplitude in L2/3 that occurred in uninjected, D-row deprived rats was absent (p < 0.05 vs deprived, unpaired t-test). In contrast, D-row deprived rats injected daily with vehicle showed normal deprivation-induced weakening of L2/3 WEPs (−0.37 ± 0.06 mV, n = 8, p < 0.05 vs. control), and the same non-significant trend towards weakening of L4 WEPs as in uninjected rats (−0.68 ± 0.04 mV, n = 8, p > 0.05 vs. control). WEP recording locations were similar for these different animal groups (Fig. 7B). Identical results were obtained for WEP slope (data not shown). Enhanced WEPs in deprived columns were not due to general boosting of sensory responses by AM251, or to inadvertent differences in anesthetic state or WEP electrode recording characteristics, because the amplitude of WEPs in L2/3 evoked by neighboring, spared whiskers in their home columns in these same animals was identical in AM251-treated vs. vehicle-treated animals (vehicle: −0.68 ± 0.10 mV; AM251: −0.62 ± 0.11 mV, n = 8 each, p = 0.7). Thus, CB1 receptor signaling is required for rapid depression of responses to deprived whiskers in L2/3 of their home columns in vivo, measured by WEPs.

Selectivity of AM251 and acute effects on cortical sensory responses

To determine if the effects of AM251 on map development and plasticity were secondary to gross changes in cortical activity, we characterized the acute effect of systemic AM251 on sensory responses of L2/3 neurons in urethane anesthetized rats. AM251 (5 mg/kg, i.p.) did not alter single-unit spiking responses to principal whisker deflection (before injection: 0.38 ± 0.05 spikes per stimulus, 1 hr after: 0.41 ± 0.05, p = 0.4, paired t-test), indicating that sensory responsiveness was not grossly perturbed (n = 19 single units, 4 recording sites, 4 animals) (Fig. S6A). AM251 mildly increased spontaneous firing rate (before: 0.83 ± 0.13 Hz, 1 hr after: 1.2 ± 0.18 Hz, p < 0.009, paired t-test) and surround whisker responses (mean response to the 4 immediate surround whiskers, before: 0.12 ± 0.08 spikes stimulus^{-1}; after: 0.20 ± 0.10, p < 0.02, paired t-test). At a higher dose (10 mg/kg), AM251 injection acutely increased peak WEP amplitude evoked by principal whisker deflection (normalized amplitude, before: 100 ± 4.0, 1–2 hr after: 148 ± 6.7, n = 3 rats, p < 0.01, t-test) (Fig. S6B). These findings are consistent with mouse visual cortex, where AM251 injection increases the amplitude of VEPs, but not single-unit visual responses, for 12 hr after injection (Liu et al., 2008). Thus, AM251 has relatively modest effects on sensory responsiveness of cortex, though additional effects including changes in inhibitory-excitatory balance or spike timing cannot be excluded.

In vitro, AM251 is CB1-selective, with > 300-fold higher IC_{50} at related receptors (CB2, TRPV1). To test selectivity in the whisker pathway in vivo, we assayed for acute effects of AM251 injection on WEPs in constitutive CB1 receptor knockout mice (Marsicano et al., 2002). Unlike in rats, AM251 injection (10 mg/kg, i.p.) had no effect on WEPs in CB1 knockout mice, consistent with selective action at CB1 receptors (Figure S6).

Critical period for CB1 dependence of map development and plasticity

To test for a critical period for CB1 receptor involvement in map development, we administered AM251 (5 mg/kg) or vehicle daily starting at P26–30, for 7 days. Whisker receptive fields were mapped 1 d after final injection, at P34–38. Whisker receptive field maps were normal in these “Late AM251” animals (Figure 8A). Across all penetrations (including both L4 and L2/3 sites,

column edges and centers), median P(correct tuning) was 100% in Late AM251 cases (n = 14 penetrations), 88% for vehicle controls (n = 38, $p < 0.78$, Wilcoxon test) and 100% for normal, uninjected age-matched controls (n = 18, $p < 0.50$) (Figure 8B). Column edges showed normal whisker tuning [Late AM251, median P(correct tuning): 75%, n = 7; vehicle: 94%, $p > 0.05$, Wilcoxon test], as did column centers (Late AM251: 100%, n = 7; vehicle: 88%, $p > 0.05$). Normal tuning was found in both L2/3 [Late AM251, median P(correct tuning): 100%, n = 14; vehicle: 100%, n = 38, $p < 0.73$] and L4 (Late AM251: 100%, n = 14; vehicle: 100%, n = 38, $p < 0.16$). Thus, blocking CB1 receptors starting at P26 did not blur the whisker map.

To test for a critical period for CB1 receptor involvement in map plasticity, we trimmed D-row whiskers for 3 days starting at P33, and recorded WEPs in D1 and D2 columns in vivo (Figure 8C). This late D-row deprivation significantly reduced L2/3 WEP amplitude, by 39%, relative to age-matched control rats with normal whisker experience (D-row deprived, peak WEP amplitude: -0.46 ± 0.01 mV, n = 7; control: -0.76 ± 0.11 mV, n = 6; $p < 0.04$, t-test). L4 WEPs were reduced somewhat less, by 34% (D-row deprived: -0.75 ± 0.06, n = 7; control: -1.14 ± 0.08 mV, n = 6 $p < 0.01$). Unlike in younger animals, daily AM251 treatment during trimming failed to block the reduction in WEP amplitude in either L2/3 (AM251: -0.30 ± 0.04 mV, n = 7; $p < 0.01$ vs control; $p > 0.05$ vs uninjected D-row deprived) or L4 (AM251: -0.81 ± 0.03 mV, n = 7; $p < 0.01$ vs. control; $p > 0.05$ vs uninjected D-row deprived). WEP amplitude was also reduced in D-row deprived rats injected daily with vehicle (L2/3: -0.43 ± 0.07 mV, n = 6; $p < 0.03$ vs. control; L4: -0.76 ± 0.12 mV, n = 6, $p < 0.04$ vs. control). Thus, CB1 receptor signaling is required for weakening of deprived whisker responses at P19, but not at P33.

Discussion

How sensory experience guides neural circuit formation is a long-standing question in neuroscience. Most models posit early, activity-independent mechanisms for synapse formation and targeting, followed by NMDA receptor-dependent, Hebbian plasticity that alters initial circuits according to activity and experience (e.g., Katz and Shatz, 1996). Recently, multiple forms of CB1-dependent plasticity have been discovered, including transient weakening of inhibitory and excitatory synapses (DSI and DSE) and CB1-LTD, which implements long-lasting, Hebbian synapse weakening (Chevaleyre et al., 2006). In these forms of plasticity, activity triggers postsynaptic release of endocannabinoids, which diffuse retrogradely to activate presynaptic CB1 receptors, which decreases transmitter release probability. DSI, DSE, and CB1-LTD occur at many synapses in vitro, including in primary sensory cortex (Trettel and Levine, 2002; [2003]; Sjostrom et al., 2003; Bender et al., 2006b; Crozier et al., 2007). By regulating both inhibition and excitation, CB1-mediated plasticity has a potentially powerful role in regulating circuit computation, excitability, and in gating activity-dependent synaptic plasticity. Whether CB1-mediated plasticity contributes to systems-level development and plasticity in vivo is unknown.

We found that treatment with the CB1 receptor antagonist AM251 during early postnatal whisker map development caused S1 neurons to develop abnormal whisker receptive fields that included strong responses to inappropriate whiskers, and also prevented deprivation-induced weakening of synapses and whisker sensory responses. CB1 receptors are likely to be the relevant target for AM251 in the whisker pathway, because AM251 is >300-fold selective for CB1 receptors over CB2 receptors (Gatley et al., 1997; Lan et al., 1999), is inactive at other known cannabinoid-sensitive receptors including TRPV1 and putative CB3 (Hajos and Freund, 2002; Mackie and Stella, 2006; Gibson et al., 2008), and because the acute effect of AM251 on WEPs was abolished in CB1 knockout mice (Figure S6). Thus, these results implicate CB1 receptors (or, potentially, an undiscovered alternate target of AM251) in weakening of synapses and sensory responses during early postnatal development of the S1 whisker map. CB1 involvement could not be confirmed using CB1 knockout mice, because these mice develop

compensatory forms of synapse weakening (V.A. Bender, D.R.C. House, D. E. Feldman, unpublished results).

CB1 regulation of map development

Postnatal day 12–15 is a period of robust synaptogenesis, maturation of whisker responses, and experience-dependent plasticity in S1 (Glazewski et al., 1996; Micheva and Beaulieu, 1996; Stern et al., 2001; Bender et al., 2003; Bureau et al., 2004). CB1 blockade during and just after this period disrupted formation of the whisker map, with neurons in barrel column edges developing abnormally strong responses to inappropriate whiskers, resulting in mistuned single-unit whisker receptive fields, and fractured, blurred whisker maps. Disruption was greatest in L2/3 and modest in L4, mirroring the laminar expression of CB1 receptors and CB1-dependent plasticity in vitro (Trettel & Levine, 2002; [2003]; Bodor et al., 2005; Deshmukh et al., 2007; Bender et al., 2006b), and indicating a primary locus for map disruption in intracortical circuits. Candidate circuit mechanisms include failure to prune excitatory L4-L2/3, L2/3-L2/3 or other cross-columnar circuits, which could drive inappropriate responses at column edges; decreased or delayed inhibition, which normally suppresses surround whisker responses (Kyriazi et al., 1996; Foeller et al., 2005); or development of inappropriate inputs to L2/3 from L4 septa (Shepherd et al., 2003).

What CB1-dependent cellular mechanisms are involved is not clear. In an activity-independent model, CB1 blockade may disrupt CB1 regulation of target selection by growing axons (Berghuis et al., 2007; Mulder et al., 2008). In an activity-dependent model, inappropriate synapses may be functionally weakened during this period by CB1-dependent plasticity (presumably CB1-LTD), which may also contribute to the robust experience-dependent plasticity at this age (Glazewski et al., 1996; Lendvai et al., 2000; Stern et al., 2001; Broser et al., 2008; Bruno et al., 2009). In this model, CB1 blockade would cause inappropriate responses to non-principal whiskers to be maintained, generating imprecise, broad whisker tuning. Alternatively, DSI or DSE may sculpt cortical spiking activity to enable activity-dependent refinement of developing circuits, which would be prevented by CB1 blockade. This model may be less likely since AM251 injection only modestly altered gross spiking activity and WEPs in S1 (Figure S6), similar to visual cortex (Liu et al., 2008), though subtle changes in spike pattern, or changes only apparent during awake behavior, may be sufficient to disrupt plasticity. Map disruption is unlikely to reflect deficits in general growth, because AM251-treated rats gained weight steadily, though somewhat more slowly than control rats.

CB1 receptors in experience-dependent plasticity

L4-L2/3 excitatory synapses are a known site of experience-dependent plasticity in S1 (Feldman, 2009). Whisker deprivation weakens L4-L2/3 synapses, and this has been proposed to drive the loss of deprived whisker responses in L2/3, which is a rapid component of juvenile map plasticity (Glazewski et al., 1996; Wallace & Fox, 1999; Foeller et al., 2005; Drew et al., 2008). Deprivation-induced weakening of L4-L2/3 synapses may represent CB1-LTD, because CB1-LTD is robust at these synapses in vitro (Bender et al., 2006b), both deprivation and CB1-LTD weaken synapses presynaptically (Bender et al., 2006a; 2006b), and deprivation-induced weakening occludes CB1-LTD (Allen et al., 2003; Crozier et al., 2007). We found that AM251 treatment prevented deprivation-induced weakening of L4-L2/3 synapses as assayed by increased paired pulse ratio in ex vivo brain slices, and prevented weakening of L2/3 whisker responses in vivo as measured by WEPs (Fig. 6, Fig. 7). Thus, CB1 receptors are required for rapid weakening at L4-L2/3 synapses, and for loss of responses to deprived sensory inputs in L2/3. These findings are consistent with the model that CB1-LTD mediates these components of plasticity in vivo. Other models include CB1 signaling being indirectly permissive for plasticity (e.g., if DSI or DSE normally set appropriate spiking patterns or inhibitory tone required for plasticity, or if CB1 receptors regulated the animal's behavioral or

neuromodulatory state). Distinguishing these models will require molecular tools that selectively disrupt specific forms of CB1-dependent plasticity.

We used WEPs to assess plasticity because WEPs are rapidly depressed by whisker deprivation (3 days), compared to whisker-evoked spike counts, which depress more slowly (7 days; Glazewski et al., 1996; Li and Feldman, data not shown). Thus WEPs allow rapid mechanisms of map plasticity to be studied. Reduction of WEP amplitude in L2/3 but not L4 or L5a is consistent with a locus of rapid plasticity in L2/3, and with rapid deprivation-induced weakening of L4-L2/3 synapses (Fig. 6) (Drew et al., 2008). CB1 signaling was required for rapid weakening of WEPs. Whether slower components of plasticity, including reduction in L2/3 spiking responses, also require CB1 signaling remains unknown.

In a recent paper, Liu and colleagues (2008) showed that CB1 blockade prevented weakening of closed-eye visual responses in L2/3 of mouse V1 during ocular dominance plasticity, and concluded that CB1 receptors are required for rapid weakening of deprived sensory inputs. Our results extend this conclusion to S1, and show that L4-L2/3 excitatory synapses are a specific site of CB1-dependent synapse weakening in vivo. In addition, we found that normal development of whisker receptive fields was disrupted by CB1 blockade, suggesting that CB1-dependent synapse weakening contributes to normal circuit development. However, whether CB1 receptors influence map development and plasticity via the same mechanism remains unknown.

CB1 signaling was required for whisker map development and plasticity only during an early critical period ending before P26. This indicates that distinct, non-CB1-dependent mechanisms exist for weakening deprived whisker representations and maintaining map topography after this age. These mechanisms may include classical postsynaptic LTD based on GluR1 internalization (Wright et al., 2008; Yoon et al., 2009), or other forms of synapse regulation and structural plasticity (Lendvai et al., 2000; Shepherd et al., 2003; Maffei and Turrigiano, 2006; Cheetham et al., 2008). We speculate that the transition from CB1-dependent to CB1-independent map plasticity in S1 reflects developmental downregulation of CB1-dependent synaptic plasticity at key S1 synapses.

Experimental Procedures

All experiment procedures were approved by UCSD and UC Berkeley Institutional Animal Care and Use Committees and are in accordance with NIH guidelines. Long-Evans rats (both genders) were used. Constitutive CB1 receptor knockout mice (Marsicano et al., 2002) were used for experiments in Fig. S6 (kindly provided by G. Marsicano & B. Lutz, Univ. Mainz, Germany).

Whisker deprivation

Right-side D-row (D1–D6) and γ whiskers were plucked (for in vitro slice experiments) or trimmed to the base (for in vivo WEP experiments) under isoflurane anesthesia (3% in 2 L/min O_2). Both trimming and plucking drive depression of deprived whisker representations in L2/3 in vivo (Drew and Feldman, 2008). Trimming was required for WEP experiments to allow deflection of trimmed whisker stubs to elicit WEPs. Sham-deprived littermates were anesthetized and handled identically, but not plucked/trimmed.

AM251 and Vehicle administration

AM251 was suspended (5 or 10 mg/kg) in vehicle solution (10% Tween 80 in sterile deionized water) and vortexed immediately before i.p. injection. In order to minimize weight loss associated with CB1 blockade (DiMarzo et al., 2001), 0.5 mL lactated Ringer solution was co-

administered beginning on the second day, for both AM251 and vehicle injections. Recording started 24 hr after the last injection.

Surgery

Surgical methods were as published (Drew and Feldman, 2008). Briefly, Long-Evans rats (P33 – P36) were anesthetized with urethane (1.5 g/kg, 20–30% in sterile saline, i.p.) and a craniotomy made over left S1 (5.5 mm lateral, 2.5 mm posterior to Bregma). The skull was thinned for optical imaging or removed to expose the dura for electrophysiological recording. The brain was kept moist with saline.

Intrinsic signal optical imaging

Reflectance images were acquired through the thinned skull under red light illumination (630 nm), focused 400–600 μm underneath the pia, as described previously (Drew and Feldman, 2008). Three whiskers (either E1, D1 and C1, or E2, D2 and C2) were stimulated in alternation to identify the whisker response area (WRA) for each whisker. Blood vessel artifacts extending out of a WRA were masked prior to WRA area calculation (Drew and Feldman, 2008).

Extracellular recording and mapping

Multi-unit extracellular recording was performed with tungsten electrodes (~5 MΩ at 1 kHz; FHC, Bowdoinham, ME) advanced through a slit in the dura. Penetration angle was adjusted to be radial by advancing two equal-length, laterally spaced (100 μm) electrodes, and verifying simultaneous contact of both tips with the cortical surface. Recordings were made 200 – 970 μm below the pia (radial spacing > 50 μm). Recordings were made at 3000× gain, 0.5–3 kHz bandpass, digitized at 32 kHz at 12-bit resolution. Multiunit spikes (amplitude > 7 s.d. above noise) were isolated off-line. Whisker responses were quantified 100 ms after deflection onset, with spontaneous firing subtracted (100 ms before deflection). At each recording site, nine whiskers in a 3 × 3 grid were deflected in random, interleaved order (20 – 30 repetitions each) to construct a whisker tuning curve. The empirical PW was defined as the whisker that evoked the greatest number of spikes (for equal responses, the shorter latency whisker was designated PW). For display, tuning curves are shown as gaussian filtered, 3 × 3 grids, normalized to the empirical PW response. During recording, anesthesia was maintained with supplemental urethane (10% of original dose, i.p.), and body temperature was maintained at 37°C.

Localization of recording sites to L2/3 or L4 was determined by microdrive depth readings (200–600 and 600–900 μm below the pia, respectively), following experiments in which marking lesions were made at defined microdrive depths and recovered in CO-stained coronal sections (Fig. S1). The exact number of L2/3 and L4 recording sites varied across penetrations, but the overall proportion of L2/3 sites was similar between groups (AM251: 54%; vehicle: 47%; control: 51%).

A subset of penetrations (3 – 4) was marked by electrolytic lesions in L4 (2.8 μA, 10 s), which were recovered in tangential sections stained for cytochrome oxidase to reveal the barrels. In some experiments, lesions were made after completion of all recording penetrations by returning to earlier penetration sites, as marked by microdrive coordinates and surface blood vessels; in other experiments, lesions were made upon completion of individual penetrations. These strategies produced identical results. Additional lesions marked the rostrocaudal or mediolateral axis. Location of other penetrations was calculated by interpolation from microdrive coordinates. Only penetrations localized to barrels were analyzed.

For single-unit recording experiments, extracellular activity was recorded following the same protocol as for multi-unit recording. Single-unit spikes (threshold amplitude 5–10 s.d. above noise; peak amplitude 20 – 100 μV) were isolated offline using a non-Gaussian clustering-

based, semi-automated spike sorting algorithm (Fee et al., 1996). 67/75 (92%) of single units had spike waveforms with total spike width (initial positive and subsequent negative deflection) > 0.7 ms, consistent with regular spiking, putative excitatory neurons (Swadlow, 1989; Armstrong-James et al., 1993). The proportion of regular spiking units was 96% (49/51) in AM251 cases and 84% (20/24) in control cases.

For WEP recording, glass microelectrodes (1.8 MΩ, ranging between 1.7 and 1.9 MΩ), filled with Ringer solution) were manufactured and stored in batches with closely matched tip size and resistance (2.2 ± 0.1 MΩ for WEP recording in young animals). WEPs were recorded with an Axopatch-200B amplifier (200 gain, 2 kHz lowpass filter, sampled at 5 kHz). Trimmed D-row whisker stubs (~ 3 mm length) were deflected to evoke WEPs.

Whisker Stimulation

Nine independent, computer-controlled piezoelectric bimorph elements (T215-H4CL-103X, 1.25" × 0.125" × 0.015"; Piezo Systems, Cambridge, MA) were used to deliver ramp-hold whisker deflections (2°, 4 ms ramp/return, 100 ms hold for unit recordings, 60 ms hold for intrinsic signal imaging, applied 5 mm from the face, corresponding to 62.5 mm/s (550°/s) deflection velocity). Whiskers were glued in lightweight plastic tubes attached to the piezo elements. Piezo movement was calibrated optically to produce minimal ringing (ringing was < 5% of total displacement amplitude) and independence between piezos (attenuation > 20 dB between neighboring elements).

Slice electrophysiology

Rats (P19 – 22) were anesthetized with isoflurane, decapitated, and the brain was removed in chilled Ringer's solution (in mM: NaCl, 119; KCl, 2.5; $MgSO_4$, 1.3; NaH_2PO_4, 1; $NaHCO_3$, 26.3; D-(+)-glucose, 11; and $CaCl_2$, 2.5, bubbled with 95% O_2/5% CO_2 [pH 7.4]). "Across row" S1 slices (400 μm) containing one barrel column from each whisker row (A – E) were cut from the left hemisphere 50° from the midsagittal plane. Slices were incubated in Ringer's solution for 30 min at 30°C, and then at room temperature for 0.5–6 h before recording.

Whisker barrels were visualized with transmitted light, and a bipolar stimulating electrode (FHC, Bowdoinham, ME) was placed in the geometric center of a L4 barrel. L2/3 pyramidal cells above the center of the stimulated barrel were visualized with infrared differential interference contrast optics, and whole-cell voltage clamp recordings were made at room temperature (22 – 24°C) using 3 – 4 MΩ pipettes and a Multiclamp 700B amplifier (Molecular Devices, Sunnyvale, CA) and custom acquisition software written in IgorPro (Wavemetrics, Lake Oswego, OR). Data were acquired at 5 kHz and filtered at 3 kHz. Internal solution contained (in mM): D-gluconic acid 118; CsOH 118; HEPES 20; EGTA 0.4;NaCl 2.8; TEA-Cl 5; MgATP 4; NaGTP 0.3; phosphocreatine 10; pH 7.20 – 7.25. R_{in} and R_s were monitored continuously. R_s was not compensated. Experiments were discarded if initial $V_m > -75$ mV, $R_s > 25$ MΩ or $R_{in} < 100$ MΩ, or if R_s or R_{in} changed by 20% during recording. All V_m values were adjusted for the measured liquid junction potential (11 mV).

Paired stimuli at 40 ms inter-stimulus intervals (ISI) were delivered every 25 sec (6 – 8 sweeps each; holding potential: −80 mV) in normal Ringer's solution. α-amino-3-hydroxy-5methyl-4-isoxazole-propionate (AMPA) receptor mediated currents were isolated with bath application of D-(−)-2-amino-5-phosphonopentanoic acid (D-AP5) (50 μM) and focal administration of bicuculline methiodide (BMI) via a pipette (5 mM BMI, 5 μm tip internal diameter, located < 100 μm from recorded cell). Paired pulse ratio (PPR) was defined as the mean amplitude of the second EPSC to the first. When the second pulse overlapped with the decay of the first, the residual current was subtracted.

Chemicals

AM251 and D-AP5 were from Tocris. All other reagents were from Sigma-Aldrich.

Statistics

P(correct tuning) values were compared across groups using nonparametric statistics including the Wilcoxon test (Mann-Whitney U test), because P(correct tuning) distributions were non-normal (Lilliefors test). In slice experiments and in vivo WEP recordings, reported numbers are mean ± standard error, and statistical significance was determined using an unpaired Student's t-test. A critical value of $p < 0.05$ was used in all tests.

Supplementary Material

Refer to Web version on PubMed Central for supplementary material.

Acknowledgments

This work was supported by NIH grant NS046652-05. We are grateful to members of the Feldman laboratory for advice.

References

Allen CB, Celikel T, Feldman DE. Long-term depression induced by sensory deprivation during cortical map plasticity in vivo. Nat Neurosci 2003;6:291–299. [PubMed: 12577061]

Alloway KD. Information Processing Streams in Rodent Barrel Cortex: The Differential Functions of Barrel and Septal Circuits. Cereb. Cortex 2008;18:979–989. [PubMed: 17702950]

Armstrong-James M, Fox K. Spatiotemporal convergence and divergence in the rat S1 "barrel" cortex. J. Comp. Neurol 1987;263:265–281. [PubMed: 3667981]

Armstrong-James M, Welker E, Callahan CA. The contribution of NMDA and non-NMDA receptors to fast and slow transmission of sensory information in the rat SI barrel cortex. J. Neurosci 1993;13:2149–2160. [PubMed: 8097531]

Bender KJ, Rangel J, Feldman DE. Development of Columnar Topography in the Excitatory Layer 4 to Layer 2/3 Projection in Rat Barrel Cortex. J. Neurosci 2003;23:8759–8770. [PubMed: 14507976]

Bender KJ, Allen CB, Bender VA, Feldman DE. Synaptic Basis for Whisker Deprivation-Induced Synaptic Depression in Rat Somatosensory Cortex. J. Neurosci 2006a;26:4155–4165. [PubMed: 16624936]

Bender VA, Bender KJ, Brasier DJ, Feldman DE. Two Coincidence Detectors for Spike Timing-Dependent Plasticity in Somatosensory Cortex. J. Neurosci 2006b;26:4166–4177. [PubMed: 16624937]

Berghuis P, Rajnicek AM, Morozov YM, Ross RA, Mulder J, Urban GM, Monory K, Marsicano G, Matteoli M, Canty A, Irving AJ, Katona I, Yanagawa Y, Rakic P, Lutz B, Mackie K, Harkany T. Hardwiring the Brain: Endocannabinoids Shape Neuronal Connectivity. Science 2007;316:1212–1216. [PubMed: 17525344]

Berrendero F, Sepe N, Ramos JA, Di Marzo V, Fernández-Ruiz JJ. Analysis of cannabinoid receptor binding and mRNA expression and endogenous cannabinoid contents in the developing rat brain during late gestation and early postnatal period. Synapse 1999;33:181–191. [PubMed: 10420166]

Bodor AL, Katona I, Nyiri G, Mackie K, Ledent C, Hajos N, Freund TF. Endocannabinoid Signaling in Rat Somatosensory Cortex: Laminar Differences and Involvement of Specific Interneuron Types. J. Neurosci 2005;25:6845–6856. [PubMed: 16033894]

Broser P, Grinevich V, Osten P, Sakmann B, Wallace DJ. Critical Period Plasticity of Axonal Arbors of Layer 2/3 Pyramidal Neurons in Rat Somatosensory Cortex: Layer-Specific Reduction of Projections into Deprived Cortical Columns. Cereb. Cortex 2008;18:1588–1603. [PubMed: 17998276]

Bruno RM, Hahn TTG, Wallace DJ, de Kock CPJ, Sakmann B. Sensory Experience Alters Specific Branches of Individual Corticocortical Axons during Development. J. Neurosci 2009;29:3172–3181. [PubMed: 19279254]

Buonomano DV, Merzenich MM. Cortical Plasticity: From Synapses to Maps. Annual Review of Neuroscience 1998;21:149–186.

Bureau I, Shepherd GMG, Svoboda K. Precise Development of Functional and Anatomical Columns in the Neocortex. Neuron 2004;42:789–801. [PubMed: 15182718]

Celikel T, Szostak VA, Feldman DE. Modulation of spike timing by sensory deprivation during induction of cortical map plasticity. Nat Neurosci 2004;7:534–541. [PubMed: 15064767]

Cheetham CEJ, Hammond MSL, McFarlane R, Finnerty GT. Altered Sensory Experience Induces Targeted Rewiring of Local Excitatory Connections in Mature Neocortex. J. Neurosci 2008;28:9249–9260. [PubMed: 18784305]

Chen-Bee CH, Polley DB, Brett-Green B, Prakash N, Kwon MC, Frostig RD. Visualizing and quantifying evoked cortical activity assessed with intrinsic signal imaging. Journal of Neuroscience Methods 2000;97:157–173. [PubMed: 10788670]

Chevaleyre V, Takahashi KA, Castillo PE. Endocannabinoid-mediated Synaptic Plasticity in the CNS. Annual Review of Neuroscience 2006;29:37–76.

Deshmukh S, Onozuka K, Bender KJ, Bender VA, Lutz B, Mackie K, Feldman DE. Postnatal development of cannabinoid receptor type 1 expression in rodent somatosensory cortex. Neuroscience 2007;145:279–287. [PubMed: 17210229]

Di Marzo V, Goparaju SK, Wang L, Liu J, Bátkai S, Járai Z, Fezza F, Miura GI, Palmiter RD, Sugiura T, Kunos G. Leptin-regulated endocannabinoids are involved in maintaining food intake. Nature 2001;410:822–825. [PubMed: 11298451]

Dobrunz LE, Stevens CF. Heterogeneity of Release Probability, Facilitation, and Depletion at Central Synapses. Neuron 1997;18:995–1008. [PubMed: 9208866]

Drew PJ, Feldman DE. Intrinsic Signal Imaging of Deprivation-Induced Contraction of Whisker Representations in Rat Somatosensory Cortex. Cereb. Cortex bhn085. 2008

Fee MS, Mitra PP, Kleinfeld D. Automatic sorting of multiple unit neuronal signals in the presence of anisotropic and non-Gaussian variability. J. Neurosci. Methods 1996;69:175–188. [PubMed: 8946321]

Feldman DE. Timing-Based LTP and LTD at Vertical Inputs to Layer II/III Pyramidal Cells in Rat Barrel Cortex. Neuron 2000;27:45–56. [PubMed: 10939330]

Feldman DE. Synaptic mechanisms for plasticity in neocortex. Annu Rev Neurosci 2009;32:33–55. [PubMed: 19400721]

Feldman DE, Brecht M. Map Plasticity in Somatosensory Cortex. Science 2005;310:810–815. [PubMed: 16272113]

Feldmeyer D, Lubke J, Silver RA, Sakmann B. Synaptic connections between layer 4 spiny neurone-layer 2/3 pyramidal cell pairs in juvenile rat barrel cortex: physiology and anatomy of interlaminar signalling within a cortical column. J Physiol 2002;538:803–822. [PubMed: 11826166]

Foeller E, Celikel T, Feldman DE. Inhibitory Sharpening of Receptive Fields Contributes to Whisker Map Plasticity in Rat Somatosensory Cortex. J Neurophysiol 2005;94:4387–4400. [PubMed: 16162832]

Fox K. A critical period for experience-dependent synaptic plasticity in rat barrel cortex. J. Neurosci 1992;12:1826–1838. [PubMed: 1578273]

Fox K, Schlaggar BL, Glazewski S, O'Leary DD. Glutamate receptor blockade at cortical synapses disrupts development of thalamocortical and columnar organization in somatosensory cortex. Proceedings of the National Academy of Sciences 1996;93:5584–5589.

Fox K. Anatomical pathways and molecular mechanisms for plasticity in the barrel cortex. Neuroscience 2002;111:799–814. [PubMed: 12031405]

Gatley SJ, Lan R, Pyatt B, Gifford AN, Volkow ND, Makriyannis A. Binding of the non-classical cannabinoid CP 55,940, and the diarylpyrazole AM251 to rodent brain cannabinoid receptors. Life Sci 1997;61:191–197.

Gibson HE, Edwards JG, Page RS, Van Hook MJ, Kauer JA. TRPV1 Channels Mediate Long-Term Depression at synapses on Hippocampal Interneurons. Neuron 2008;57:746–759. [PubMed: 18341994]

Glazewski S, Giese KP, Silva A, Fox K. The role of α-CaMKII autophosphorylation in neocortical experience-dependent plasticity. Nat Neurosci 2000;3:911–918. [PubMed: 10966622]

Harkany T, Guzmbn M, Galve-Roperh I, Berghuis P, Devi LA, Mackie K. The emerging functions of endocannabinoid signaling during CNS development. Trends in Pharmacological Sciences 2007;28:83–92. [PubMed: 17222464]

Herkenham M, Lynn AB, Little MD, Johnson MR, Melvin LS, de Costa BR, Rice KC. Cannabinoid receptor localization in brain. Proceedings of the National Academy of Sciences of the United States of America 1990;87:1932–1936. [PubMed: 2308954]

Hájos N, Freund TF. Pharmacological separation of cannabinoid sensitive receptors on hippocampal excitatory and inhibitory fibers. Neuropharmacology 2002;43:503–510. [PubMed: 12367597]

Inan M, Crair MC. Development of Cortical Maps: Perspectives From the Barrel Cortex. Neuroscientist 2007;13:49–61. [PubMed: 17229975]

Katz LC, Shatz CJ. Synaptic Activity and the Construction of Cortical Circuits. Science 1996;274:1133–1138. [PubMed: 8895456]

Kreitzer AC, Regehr WG. Retrograde signaling by endocannabinoids. Current Opinion in Neurobiology 2002;12:324–330. [PubMed: 12049940]

Kyriazi HT, Carvell GE, Brumberg JC, Simons DJ. Quantitative effects of GABA and bicuculline methiodide on receptive field properties of neurons in real and simulated whisker barrels. J Neurophysiol 1996;75:547–560. [PubMed: 8714634]

Lan R, Liu Q, Fan P, Lin S, Fernando SR, McCallion D, Pertwee R, Makriyannis A. Structure-Activity Relationships of Pyrazole Derivatives as Cannabinoid Receptor Antagonists. Journal of Medicinal Chemistry 1999;42:769–776. [PubMed: 10052983]

Lendvai B, Stern EA, Chen B, Svoboda K. Experience-dependent plasticity of dendritic spines in the developing rat barrel cortex in vivo. Nature 2000;404:876–881. [PubMed: 10786794]

Liu CH, Heynen AJ, Shuler MGH, Bear MF. Cannabinoid Receptor Blockade Reveals Parallel Plasticity Mechanisms in Different Layers of Mouse Visual Cortex. Neuron 2008;58:340–345. [PubMed: 18466745]

Mackie K, Stella N. Cannabinoid Receptors and Endocannabinoids: Evidence for New Players. AAPS J 2006;8:E298–E306. [PubMed: 16796380]

Maffei A, Nataraj K, Nelson SB, Turrigiano GG. Potentiation of cortical inhibition by visual deprivation. Nature 2006;443:81–84. [PubMed: 16929304]

Marsicano G, Wotjak CT, Azad SC, Bisogno T, Rammes G, Cascio MG, Hermann H, Tang J, Hofmann C, Zieglgansberger W, Di Marzo V, Lutz B. The endogenous cannabinoid system controls extinction of aversive memories. Nature 2002;418:530–534. [PubMed: 12152079]

Micheva KD, Beaulieu C. Quantitative aspects of synaptogenesis in the rat barrel field cortex with special reference to GABA circuitry. J. Comp. Neurol 1996;373:340–354. [PubMed: 8889932]

Mulder J, Aguado T, Keimpema E, Barabas K, Ballester Rosado CJ, Nguyen L, Monory K, Marsicano G, Di Marzo V, Hurd YL, Guillemot F, Mackie K, Lutz B, Guzmán M, Lu HC, Galve-Roperh I, Harkany T. Endocannabinoid signaling controls pyramidal cell specification and long-range axon patterning. Proceedings of the National Academy of Sciences 2008;105:8760–8765.

Nevian T, Sakmann B. Spine Ca^{2+} Signaling in Spike-Timing-Dependent Plasticity. J. Neurosci 2006;26:11001–11013. [PubMed: 17065442]

Sato TR, Gray NW, Mainen ZF, Svoboda K. The Functional Microarchitecture of the Mouse Barrel Cortex. PLoS Biology 2007;5:e189. [PubMed: 17622195]

Sawtell NB, Frenkel MY, Philpot BD, Nakazawa K, Tonegawa S, Bear MF. NMDA Receptor-Dependent Ocular Dominance Plasticity in Adult Visual Cortex. Neuron 2003;38:977–985. [PubMed: 12818182]

Shepherd GMG, Pologruto TA, Svoboda K. Circuit Analysis of Experience-Dependent Plasticity in the Developing Rat Barrel Cortex. Neuron 2003;38:277–289. [PubMed: 12718861]

Simons DJ, Carvell GE. Thalamocortical response transformation in the rat vibrissa/barrel system. J. Neurophysiol 1989;61:311–330. [PubMed: 2918357]

Stern EA, Maravall M, Svoboda K. Rapid Development and Plasticity of Layer 2/3 Maps in Rat Barrel Cortex In Vivo. Neuron 2001;31:305–315. [PubMed: 11502260]

Swadlow HA. Efferent neurons and suspected interneurons in S-1 vibrissa cortex of the awake rabbit: receptive fields and axonal properties. J Neurophysiol 1989;62:288–308. [PubMed: 2754479]

Takahashi T, Svoboda K, Malinow R. Experience Strengthening Transmission by Driving AMPA Receptors into Synapses. Science 2003;299:1585–1588. [PubMed: 12624270]

Trettel J, Levine ES. Cannabinoids Depress Inhibitory Synaptic Inputs Received by Layer 2/3 Pyramidal Neurons of the Neocortex. J. Neurophysiol 2002;88:534–539. [PubMed: 12091577]

Trettel J, Levine ES. Endocannabinoids Mediate Rapid Retrograde Signaling At Interneuron -> Pyramidal Neuron Synapses of the Neocortex. J. Neurophysiol 2003;89:2334–2338. [PubMed: 12686587]

Wallace H, Fox K. The effect of vibrissa deprivation pattern on the form of plasticity induced in rat barrel cortex. Somatosens Mot Res 1999;16:122–138. [PubMed: 10449061]

Welker C. Microelectrode delineation of fine grain somatotopic organization of (SmI) cerebral neocortex in albino rat. Brain Res 1971;26:259–275. [PubMed: 4100672]

Wilson RI, Nicoll RA. Endocannabinoid Signaling in the Brain. Science 2002;296:678–682. [PubMed: 11976437]

Woolsey TA, Van der Loos H. The structural organization of layer IV in the somatosensory region (SI) of mouse cerebral cortex: the description of a cortical field composed of discrete cytoarchitectonic units. Brain Res 1970;17:205–242. [PubMed: 4904874]

Wright N, Glazewski S, Hardingham N, Phillips K, Pervolaraki E, Fox K. Laminar analysis of the role of GluR1 in experience-dependent and synaptic depression in barrel cortex. Nat. Neurosci 2008;11:1140–1142. [PubMed: 18776896]

Zucker RS, Regehr WG. Short-term synaptic plasticity. Annual Review of Physiology 2002;64:355–405.

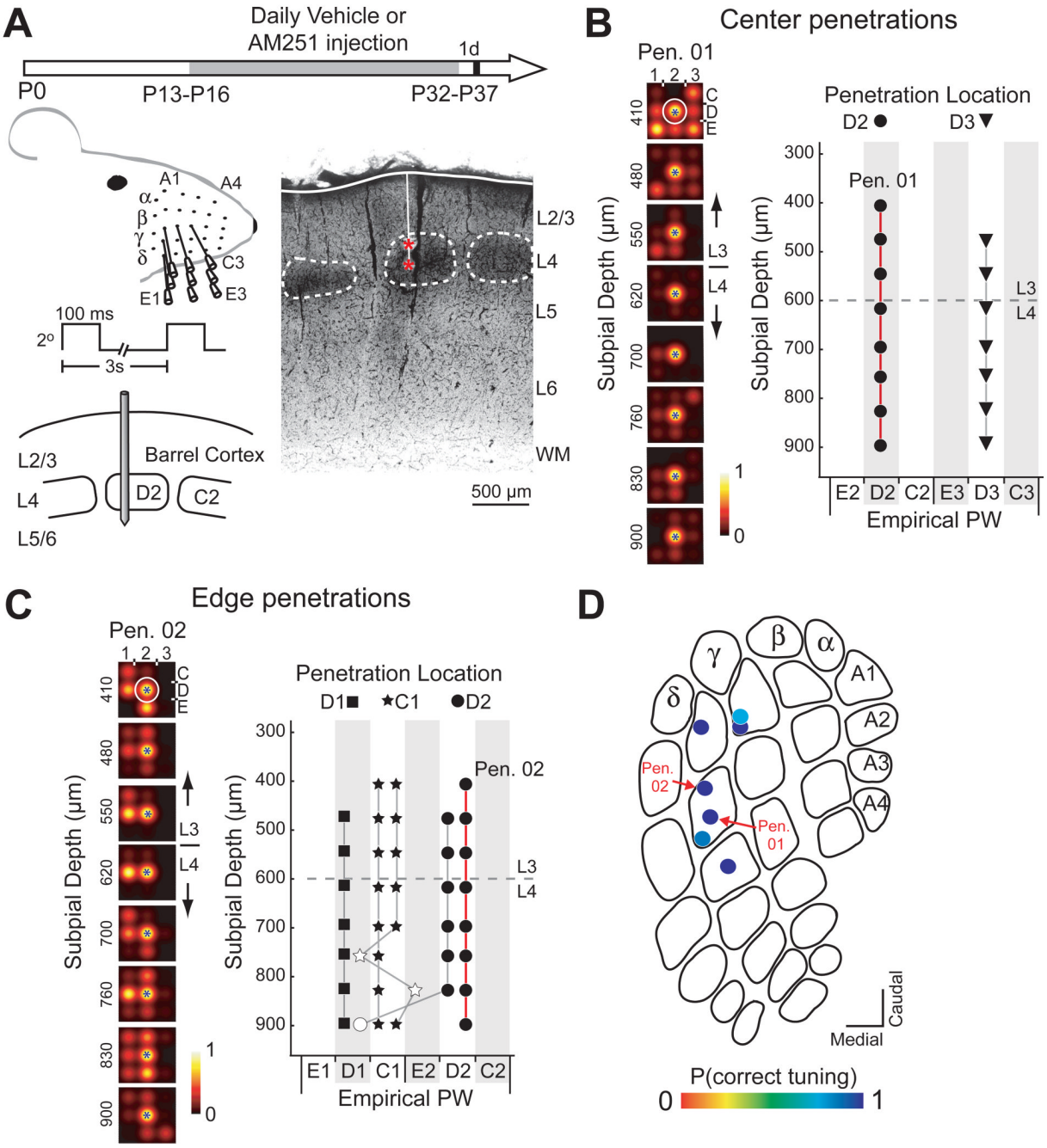

Figure 1. Whisker map precision in a vehicle-treated rat

(A) Left: Experimental design and electrophysiological recording. Right: Coronal section showing a penetration with two marking lesions (red *). Scale bar: 500 µm. (B) Multiunit receptive fields (RFs) for recording sites along a penetration through the D2 column center (PN01) in rat H46. Circle, anatomically corresponding whisker for the penetration. Blue star, measured empirical PW for each recording site. (C) Empirical PW at all recording sites in 2 center penetrations in H46. Symbol shape denotes recording site location and anatomically appropriate whisker. Filled symbols, correctly tuned sites. Dashed line, L2/3-L4 border. (D) and (E) Tuning curves and PW measured for all 5 edge penetrations in H46. Open symbols

denote mistuned sites. (F) P(correct tuning) for all penetrations in H46, plotted on an exemplar barrel map.

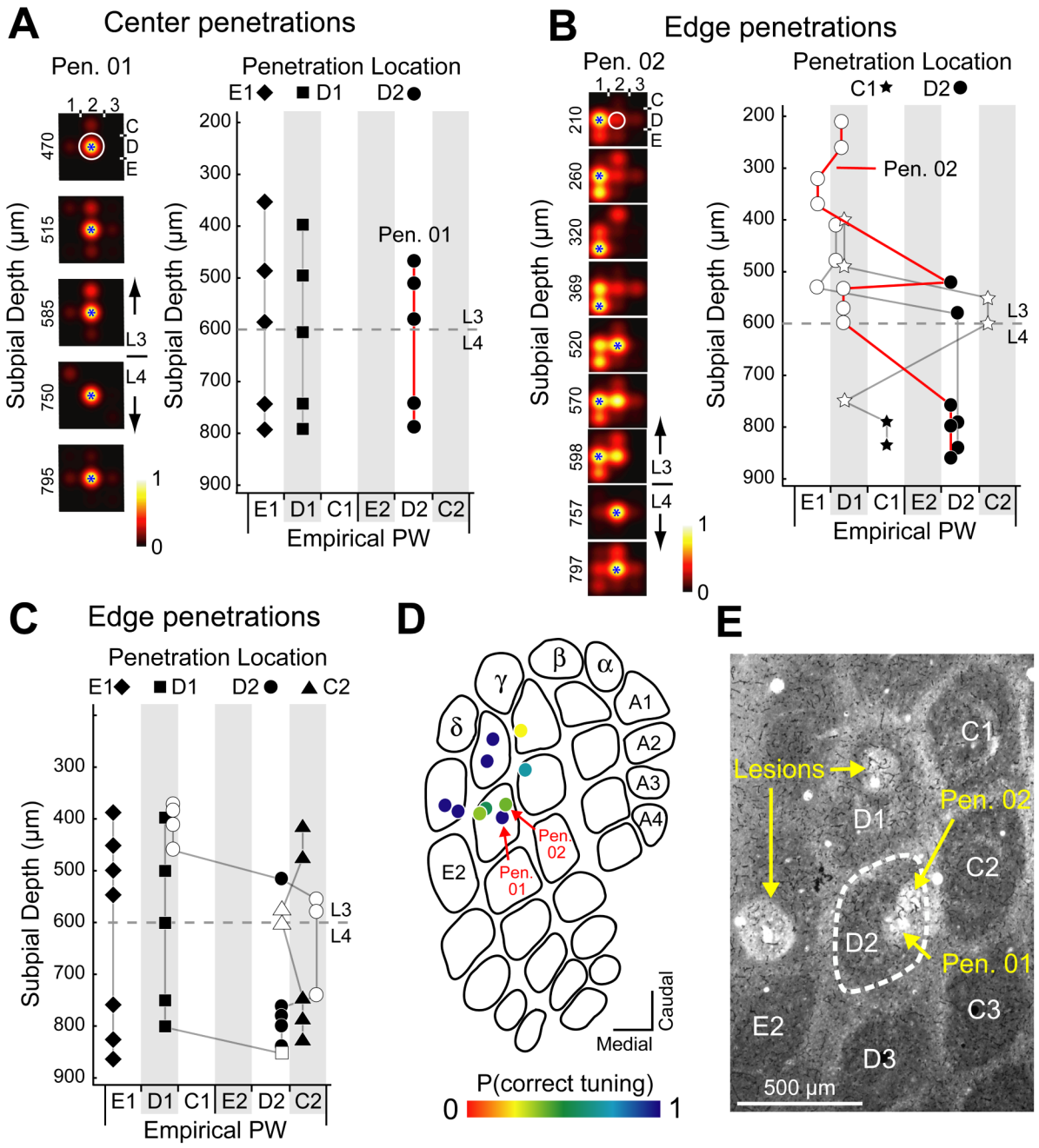

Figure 2. Disrupted whisker map in an AM251-treated rat

(A) Multi-unit whisker RFs for recording sites on a penetration through the D2 column center (Pen. 01) in AM251-treated rat H08. Circle, anatomically corresponding whisker for the penetration. Blue star, measured empirical PW for each recording site. (B) Empirical PW for recording sites in all 3 center penetrations in H08. (C) Whisker receptive fields recorded along a penetration through the D2 column edge (Pen. 02), showing many mistuned sites. (D) and (E) Empirical PW in all 7 edge penetrations in H08, showing disruption of whisker map topography. Open symbols, mistuned sites. Filled symbols, correctly tuned sites. (F) P(correct tuning) for all penetrations in H08. (G) Cytochrome oxidase-stained section showing marking lesions for Pen. 01 and Pen. 02 (arrows). D2 barrel is outlined.

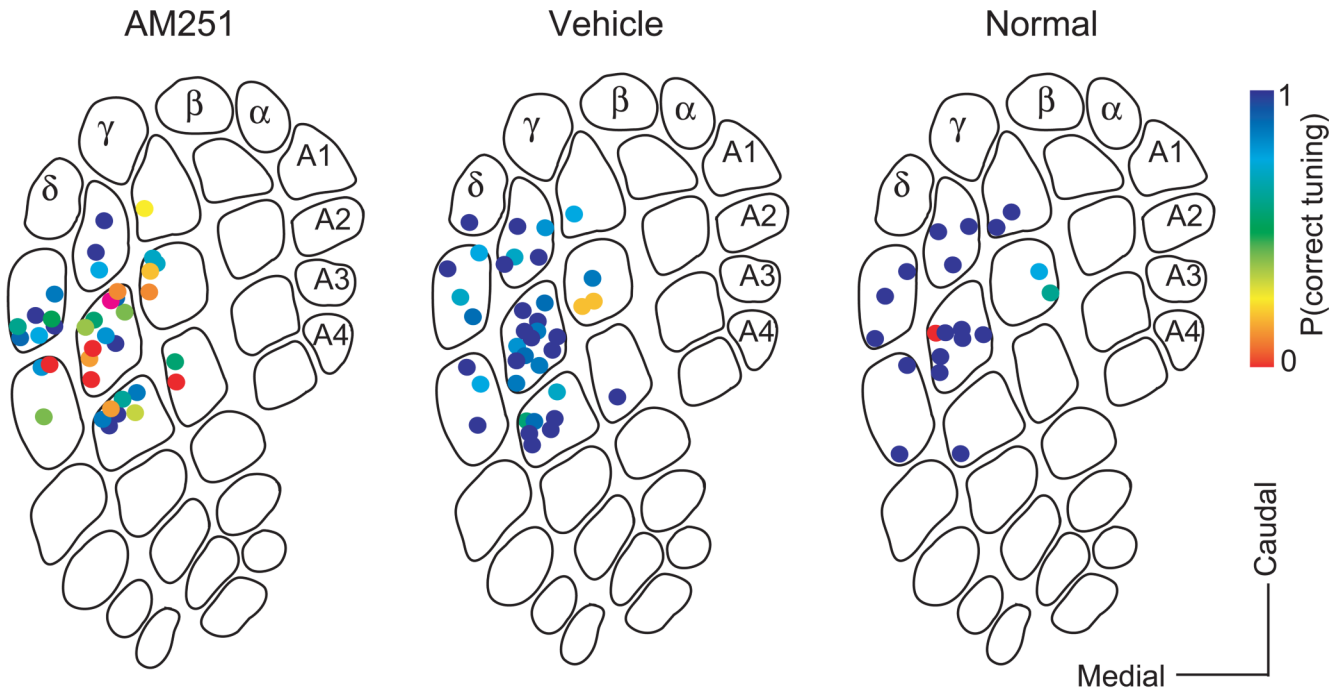

Figure 3. Whisker map precision across conditions

P(correct tuning) for all penetrations in the AM251 group (38 penetrations), vehicle control group (38 penetrations) and normal control group (20 penetrations).

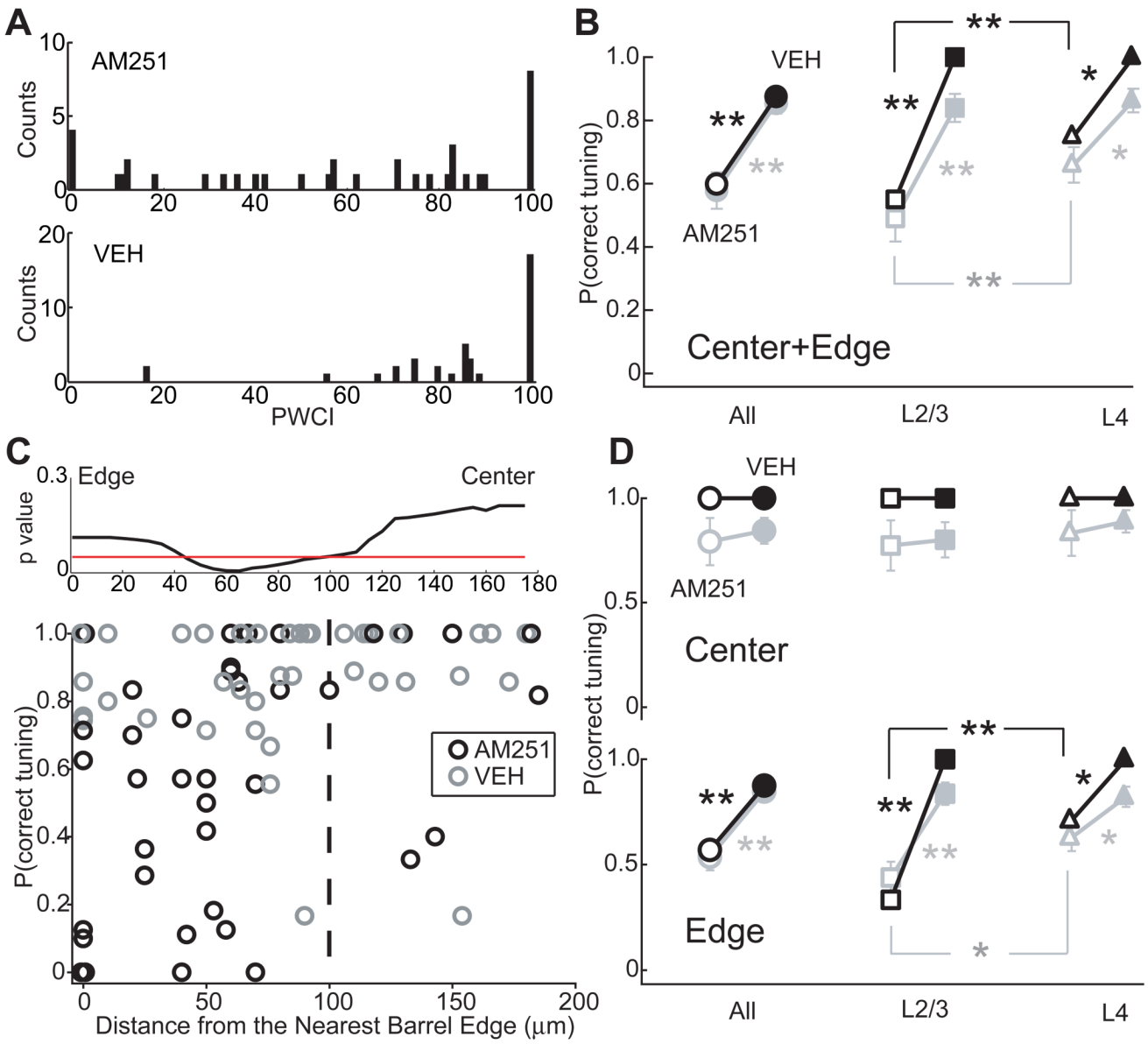

Figure 4. Quantification of laminar and sub-columnar topography of map disruption

(A) Distribution of P(correct tuning) in AM251 and vehicle control groups. (B) Median (black) and mean (gray) P(correct tuning) for the AM251 group (open symbols) and vehicle control group (filled symbols). For this and all figures, * $p < 0.05$, ** $p < 0.01$, Error bar: SEM. (C) Selective disruption at column edges. Bottom: P(correct tuning) for each penetration in AM251 (n = 38, black) and vehicle control groups (n = 38, gray) as a function of distance to the closest barrel boundary. Dashed line, center/edge border. Top: Results of sliding Wilcoxon test to identify the boundary between high- and low-P(correct tuning) regions in AM251 penetrations, data were smoothed. Red line, $p = 0.05$. (D) Median (black) and mean (gray) P(correct tuning) for penetrations in barrel centers and edges. Conventions as in (B).

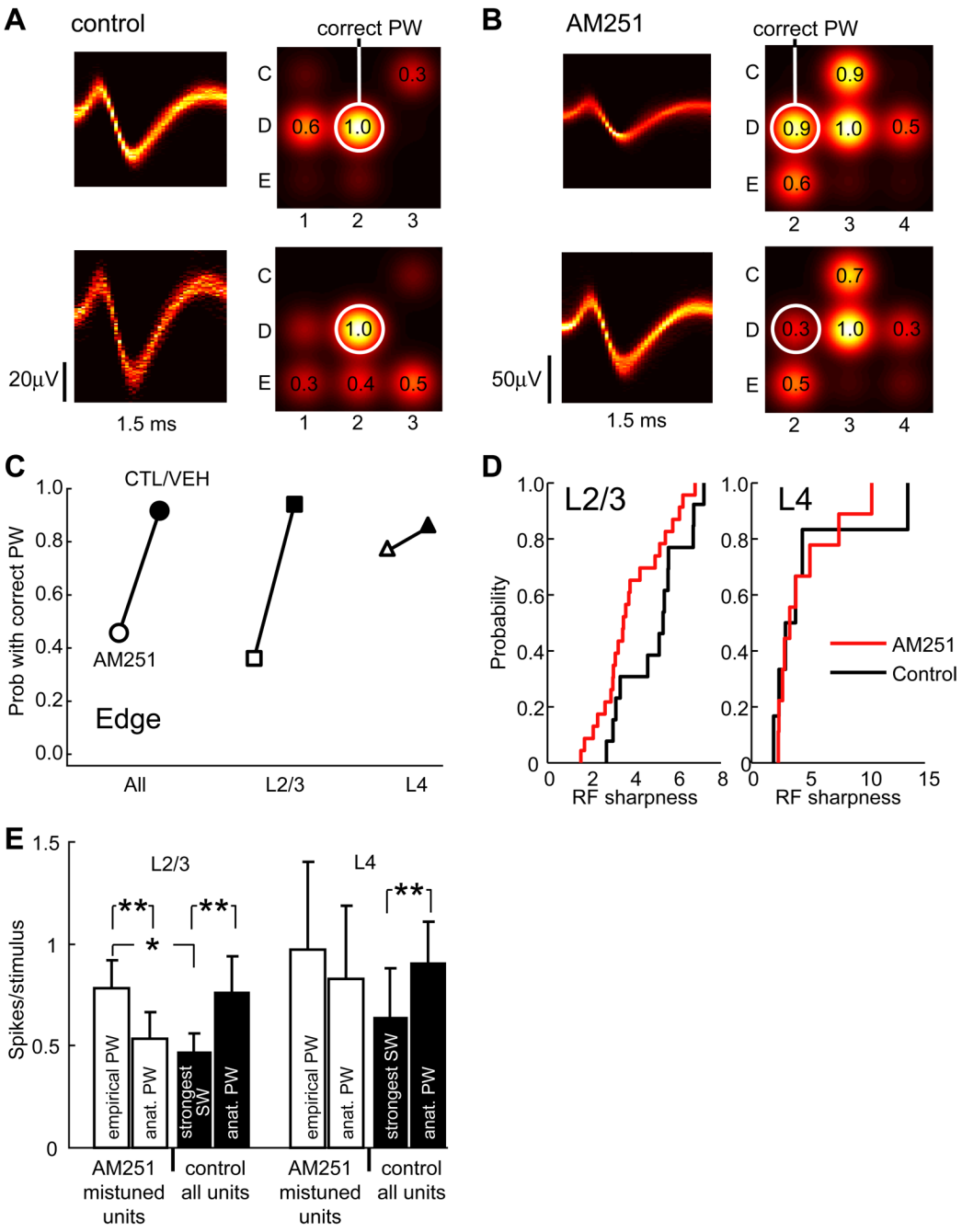

Figure 5. Disruption of single-unit receptive fields in column edges

(A) Whisker receptive fields for 2 single units in L2/3 of the D2 column edge, in a control rat. Left, density plot of spike waveform. Right, whisker receptive field (as in Fig. 1, Fig. 2), with circle marking the anatomically corresponding whisker (D2) and numbers showing response strength relative to the empirical PW. (B) Whisker receptive fields for 2 single units in L2/3 of the D2 column edge in a rat treated with AM251. These units were mistuned to the D3 whisker. (C) P(correct tuning) for all single units recorded in column edges, for AM251 animals (open) and combined control and vehicle animals (filled). (D) Cumulative distribution of receptive field sharpness. AM251 significantly broadened receptive fields in L2/3, but not L4. (E) Response magnitude (spikes per whisker deflection) for mistuned units in the AM251 group

vs. normally tuned units in the combined control/vehicle group. In mistuned units, responses to the anatomical appropriate whisker were similar to those in control units, but responses to the empirical PW were significantly stronger than responses of control cells to the strongest surround whisker.

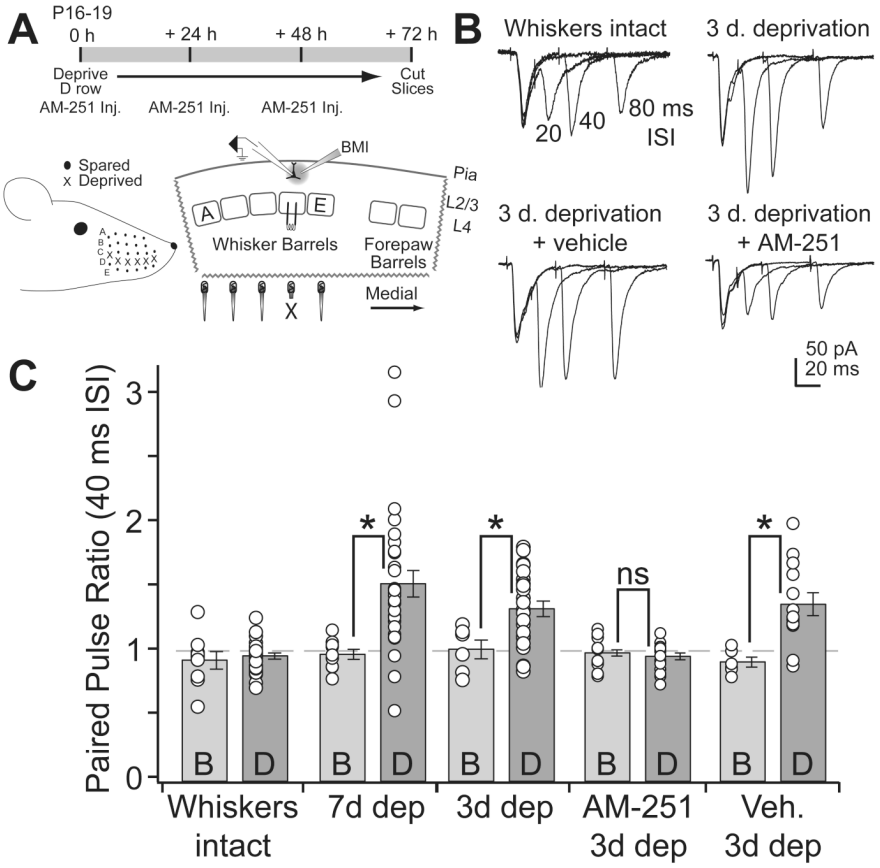

Figure 6. AM251 blocks deprivation-induced changes of paired pulse ratio at L4-L2/3 synapses

(A) Top, deprivation and drug administration timeline. Bottom, D-row whisker deprivation and positioning of stimulating and recording electrodes in the S1 brain slice. X denotes the deprived D whisker column. (B) Representative paired pulse recordings at the L4-L2/3 synapse in the D column of a control rat ("whiskers intact"), a D-row deprived rat, a D-row deprived rat that received daily vehicle injections, and a D-row deprived rat that received daily AM251 injections. Paired pulse intervals were 20, 40, and 80 ms (plotted superimposed). (C) Mean PPR at 40 ms ISI across the different experimental groups, showing results from deprived D and spared B columns within each slice. 7 d deprivation data are reprinted from Bender et al. (2006a).

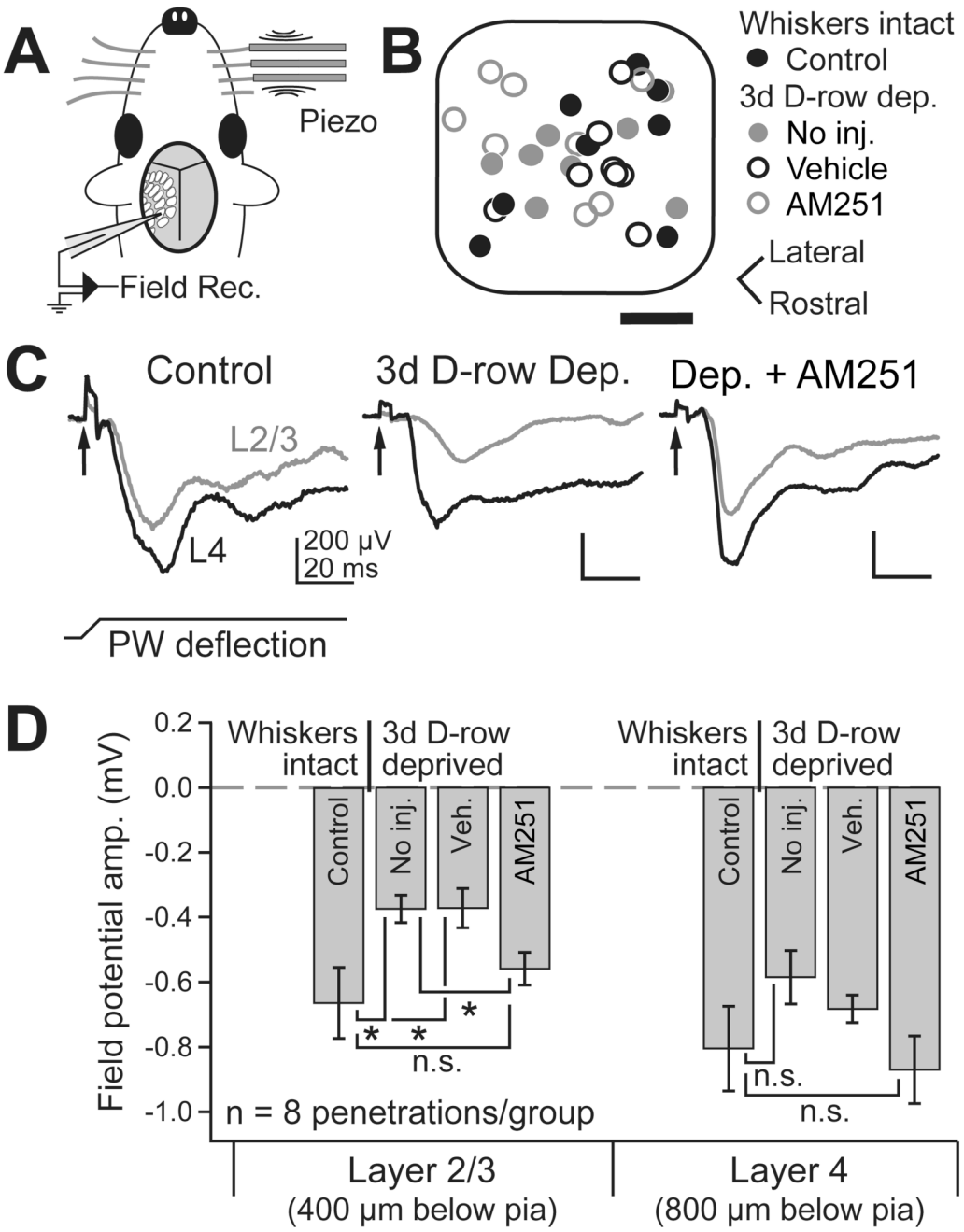

Figure 7. AM251 prevents the weakening of deprived whisker response in vivo

(A) Whisker-evoked field potential (WEP) recording methods. (B) Location of all WEP recordings, relative to normalized barrel boundaries. Scale bar, 100 µm. (C) Representative WEPs in L2/3 (grey) and L4 (black) in a control rat, a D-row deprived rat, and a D-row deprived rat that received daily AM251 injection. PW: principal whisker. Arrow, artifact marking time of whisker deflection. (D) Mean WEP amplitude for all deprivation and drug conditions.

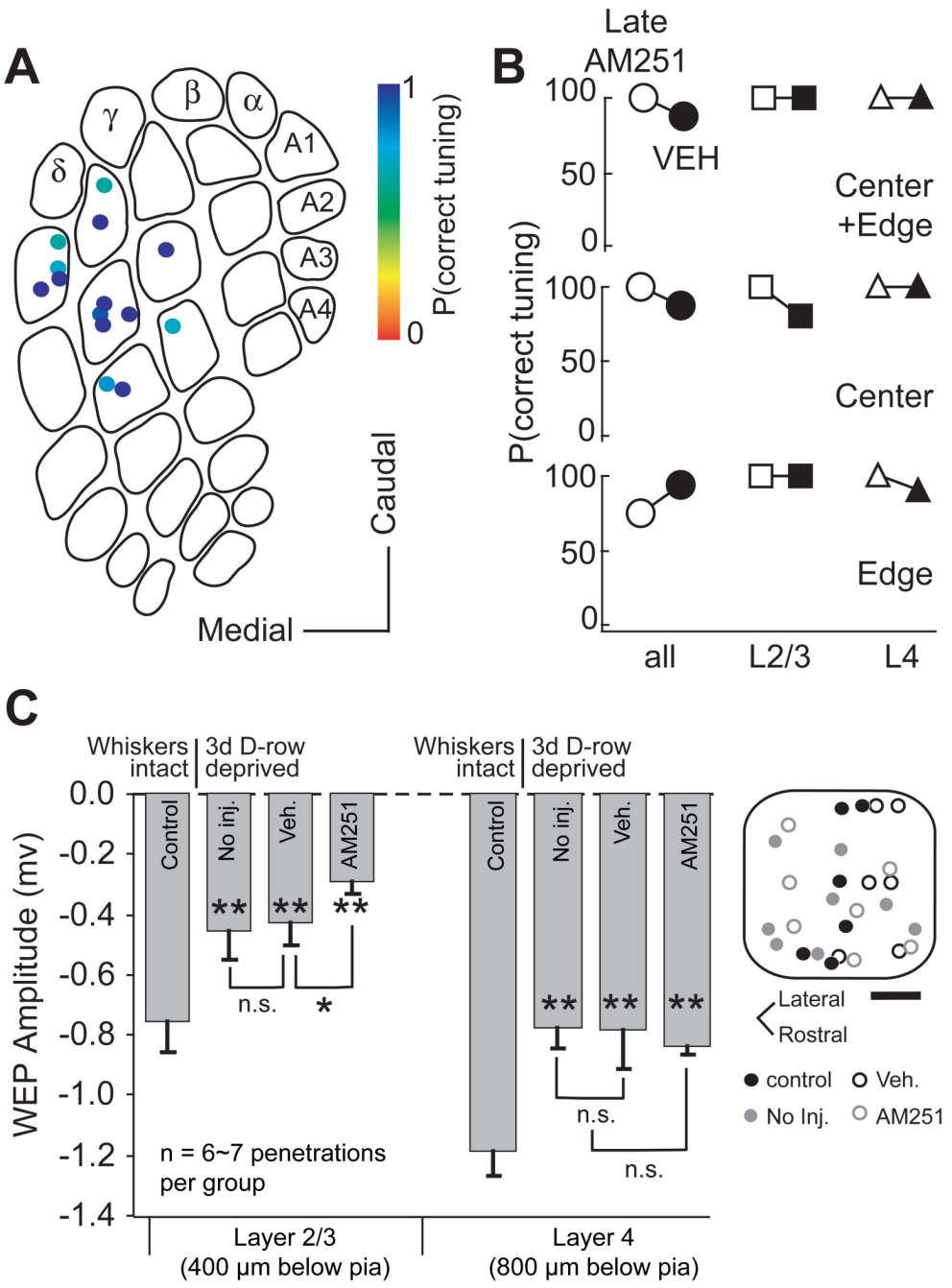

Figure 8. Critical period for eCB signaling

(A) P(correct tuning) for all penetrations in rats receiving daily AM251 (5 mg/kg) from P26–30 to P32 – 36 (Late AM251 group). (B). Median P(correct tuning) for LateAM251 group (open) and vehicle control group (filled), for edge and center penetrations, and for L2/3 vs. L4 recording sites. No significant whisker map disruption was evident. (C) Plasticity induced by D-row deprivation from P33 to 36. Bars show mean amplitude of WEPs recorded in L2/3 and L4 in control rats, D-row deprived rats, D-row deprived rats that received daily vehicle injection, and D-row deprived rats that received daily AM251 injection. AM251 did not prevent deprivation-induced weakening of WEPs in these older animals.